Passive continental margins : evidence for a prebreakup deep crustal metamorphic subsidence mechanism

Continental margin
Subsidence
Pre-breakup
Crustal metamorphism
Australia

Marge continentale
Subsidence
Pré-rupture
Métamorphisme crustal
Australie

D. A. Falvey, M. F. Middleton [a]
Department of Geology and Geophysics, University of Sydney, N.S.W. 2006, Australia.
[a] Present address : Fuel Geoscience Unit, Institute of Earth Resources, C.S.I.R.O., P.O. Box 136, North Ryde, N.S.W. 2113, Australia.

ABSTRACT

Passive continental margins in the Australian region provide evidence of very extensive sedimentation and basement subsidence both before and after the time of continental breakup. Postbreakup sedimentation is largely marine, extends to deep water and follows an exponential or thermal cooling (contraction) accumulation pattern. The pattern of prebreakup sedimentation also follows an exponential accumulation function in major depocentres, which lie en echelon, landward of the continent-ocean boundary. Here, late stage prebreakup sedimentation occurs within faulted troughs or grabens, and is described as rift phase. All prebreakup sedimentation is non marine to shallow marine, and available vitrinite reflectance data suggests deposition in a relatively low heatflow environment.

Continental crustal refraction velocities in the range 7.1 to 7.5 kms/sec. are observed beneath those margins studied, and the refractor rises markedly towards the continent-ocean boundary. The refractor is interpreted as the greenschist-amphibolite metamorphic facies boundary which has risen in response to increasing thermal conditions up until breakup time. The metamorphic conversion involves an increase in bulk density with consequent isostatic contraction which leads to subsidence and sedimentation. A quantitative basement subsidence and palaeoheatflow model has been constructed in which a simple temperature anomaly deep within the lithosphere during the prebreakup period gives rise to the observed complex subsidence pattern plus low vitrinite reflectance values.

Oceanol. Acta, 1981. Proceedings 26th International Geological Congress, Geology of continental margins symposium, Paris, 7-17 July, 1980, 103-114.

RÉSUMÉ

Marges continentales passives : présomption d'un mécanisme de subsidence prérupture de type métamorphisme crustal profond.

Les marges continentales passives d'Australie présentent une sédimentation importante ainsi qu'une subsidence du substratum tant avant qu'après la rupture du continent. La sédimentation post-rupture est surtout marine, s'effectue jusqu'en eau profonde et suit un régime d'accumulation exponentiel ou de contraction thermique. Le régime de la sédimentation pré-rupture suit aussi une loi d'accumulation exponentielle dans les zones de dépôt principales, qui s'organisent en échelon, en amont de la limite continent-océan. La dernière étape de sédimentation précédant la rupture a lieu dans des dépressions ou des grabens, et est décrite comme l'étape de distension. La sédimentation pré-rupture est de type continental à marin peu profond, et les données de vitrinite-réflectance disponibles suggèrent un dépôt dans un contexte de flux de chaleur relativement faible.

Des vitesses de réfraction de la croûte dans l'intervalle 7,1 à 7,5 km/s sont observées sous les marges étudiées et le réfracteur remonte nettement vers la limite continent-océan. Le réfracteur est interprété comme la limite des faciès métamorphiques schiste vert-amphibolite, qui est remontée en réponse à un échauffement jusqu'à l'époque de la rupture. La conversion

métamorphique implique une augmentation de la densité avec contraction isostatique, ce qui provoque la subsidence et la sédimentation. Un modèle quantitatif de subsidence du substratum et du paléoflux de chaleur a été construit, donnant à partir d'une simple anomalie de température en profondeur les régimes de subsidence complexes observés ainsi que les basses valeurs de vitrinite réflectance.

Oceanol. Acta, 1981. Actes 26ᵉ Congrès International de Géologie, colloque Géologie des marges continentales, Paris, 7-17 juil. 1980. 103-114.

INTRODUCTION

A passive continental margin evolves as a result of the breakup of continent-carrying lithosphere through seafloor spreading. In plate tectonic terms this appears to be a discrete kinematic process : the onset of significant divergent plate motion is marked by the age of oceanic crust at the continent-ocean boundary. There is no *conventional* plate tectonic evidence of pull-apart motion prior to this breakup time. The geological and structural evolution of a continental margin is however, a protracted process. For often more than 100 million years prior to breakup, major sedimentary basin subsidence may occur which is apparently influenced by the incipient line of continental separation. A complex pattern of shelf basin subsidence also occurs after breakup. These cycles of basin subsidence are termed *prebreakup* and *postbreakup* (Falvey, 1974).

In this paper we will discuss various data which support the hypothesis proposed by Falvey (1974) that prebreakup basin subsidence is due primarily to thermally induced metamorphism of the deep continental crust. A secondary, and possibly mutually exclusive mechanism may be erosional thinning of strongly elevated continental crust whose initial metamorphic grade is relatively too high. Our data suggests that marked continental crustal stretching may only occur very close to the continent-ocean boundary (beneath the deep continental lower slope) probably in the period around breakup time. Thermal cooling (lithosphere contraction) is clearly the dominant subsidence mechanism after breakup when seafloor spreading virtually removes the divergent plate boundary heat source. This process in our view only results in sediment accumulation because, by breakup time, the continental crust has been brought to near sealevel by crustal metamorphism, erosional thinning and minor stretching.

THE AUSTRALIAN CONTINENTAL MARGIN

There are more than 17,000 km of passive continental margin around Australia, formed by five distinct and well documented seafloor spreading episodes :

a) Northwest margin — Late Jurassic (155 m.y. b.p.) ;
b) Southwest margin — Early Cretaceous (120 m.y. b.p.) ;
c) Southeast margin — Late Cretaceous (80 m.y. b.p.) ;
d) Northeast margin — Early Palaeocene (65 m.y. b.p.) ;
e) Southern margin — Early Eocene (55 m.y. b.p.).

Openfile and published geological and geophysical data on all these margins have been reviewed recently by Falvey and Mutter (1981) and Veevers (1980). These summaries provide an overview of the relationships between sedimentology, structure and plate kinematics with which subsidence mechanisms may be evaluated.

Figure 1 illustrates the general, non-plateau continental margin shown by Falvey and Mutter from their review of published seismic sections of the Australian margin. Various sedimentary "units" overlie both continental and oceanic crust. The uppermost unit consists of postbreakup sediments, which are dominantly marine, transgressive shoreward and onlap oceanic crust seaward. During the immediate prebreakup period sedimentation is restricted (usually) to narrow, fault bounded grabens and half grabens arranged en echelon shoreward of the incipient continent-ocean boundary. This unit is referred to as the "rift valley phase" of prebreakup subsidence, because of the presumed morphological analogy with the East African and Red Sea rifts (Dewey, Bird, 1970 ; Falvey, 1974). Underlying this rift graben unit is a non-fault controlled, "infrarift phase" sedimentary unit. This is usually a broader, deeper, intracratonic style of basin which spans, and is elongate with respect to the incipient continent-ocean boundary.
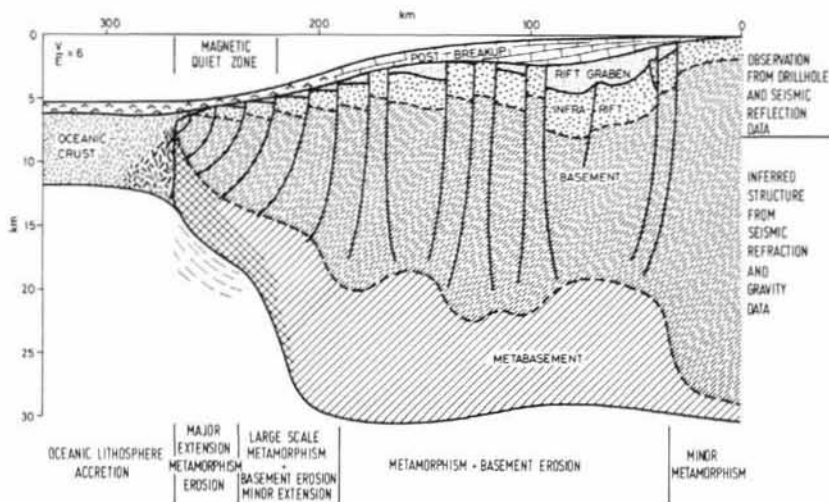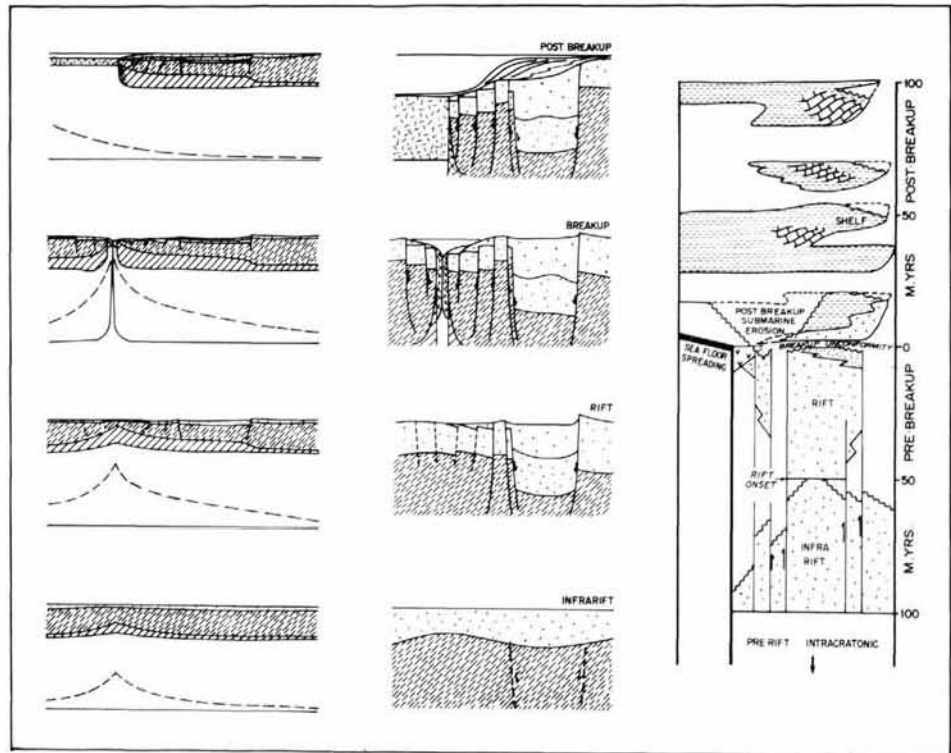

Figure 1

Generalized cross section of an Australian-type passive continental margin (after Falvey, Mutter, 1981). This section is based most heavily upon the southern, and non-plateau portions of the western margins of Australia. The infrarift, rift and postbreakup units are derived from drillhole and seismic data. The deep structure is inferred from gravity and some seismic refraction data. The only significant continental stretching which is conceded, occurs within about 50 km of the continent-ocean boundary ; along with massive crustal metamorphism and mantle underplating.

Figure 2

Right : a generalized time-stratigraphic cross section of an Australian-type passive continental margin, derived from the five specific sections in Falvey and Mutter (1981). The vertical (time) axis is in millions of years relative to breakup time. Prebreakup sediments are dominantly non-marine while postbreakup sediments quickly become marine, and transgressive shorewards. Postbreakup submarine erosion and sealevel changes are also illustrated. Centre : a sequence of generalized evolutionary cross sections of margin development. The horizontal extent is the same as the time-stratigraphic section and the vertical extent is about 10-15 km. The sequence was derived by crosscorrelating the general margin section (Fig. 1 ; and top-centre) with the general time stratigraphy. Left : a corresponding sequence of generalized lithosphere evolutionary cross sections. The horizontal extent is the same as the other sections and the vertical extent is about 100 km. These sketches describe the driving mechanism of the cycles of basin subsidence. At first, regional lithosphere heating causes some thermal uplift, then deep crustal metamorphism and infrarift basin sub-

sidence. More concentrated axial heating prevents further subsidence near the incipient continent-ocean boundary by thermal expansion outpacing metamorphism, but drives flanking rift subsidence by continued deep crustal metamorphism. After breakup, general lithosphere cooling causes postbreakup subsidence.

Falvey and Mutter also compiled a set of five time-stratigraphic cross sections derived from the hundreds of openfile exploration wells on the margin. These illustrated the depositional environments of the three major sedimentary units with respect to a spatial origin at the continent-ocean boundary, and an origin in time at breakup. A generalized abstract of these time-stratigraphic cross sections, with respect to such origins, is shown on the right hand side of Figure 2.

Correlation of this time-stratigraphic cross section with a generalized margin structural cross section (Fig. 1 ; top centre Fig. 2) leads us to suggest the evolutionary sequence of structural cross sections shown in the centre of Figure 2. These diagrammatic sections encompass those features most commonly observed on the Australian continental margin :

1) Subsidence begins with the infrarift phase (usually about 100 m.y. before breakup) preceded by some erosion of basement or prerift sediments. The infrarift basin grows along the incipient continent-ocean boundary. It does not appear to be fault controlled and contains mostly non-marine and non-volcanic sediments ;

2) from as much as 50 m.y. before breakup, through to breakup time, basin subsidence continues only in rift grabens and half grabens flanking the incipient continent-ocean boundary. Sediments are marginal to non-marine. Some volcanism is present close to the incipient continent-ocean boundary but is absent from most major depocentres in the Australian region. Some uplift and erosion of infrarift

phase sediments is evident away from the major depocentres. There is no specific evidence that any of the en echelon rift grabens are interconnected by transform or transcurrent faults. Thus there is no direct evidence of lithosphere pull-apart.

3) from breakup time, subsidence becomes widespread. Bathyal sediments are deposited at the continent-ocean boundary and onlap progressively younger oceanic crust. A marine transgression extends shoreward. Shelf and slope deposition is commonly interupted by massive submarine erosion caused by changing current patterns in the progressively widening and deepening ocean basin (Deighton *et al.*, 1976).

CONTINENTAL MARGIN SUBSIDENCE PATTERNS

The definition of infrarift, rift and postbreakup sedimentary units may be quantified by analysis of cumulative sedimentation patterns (Geohistory diagrams of Van Hinte, 1978). We have preferred this form of data presentation to the sediment stripped subsidence curves of Watts and Ryan (1976), because it cannot be assumed that sedimentation has no non-isostatic feedback effect on the driving mechanism of subsidence.

Figure 3 shows the "true" cumulative subsidence patterns of the total depth (T.D.) reached in five exploration wells on the Southern continental margin of Australia. The cumulative subsidence of higher levels in these wells have been
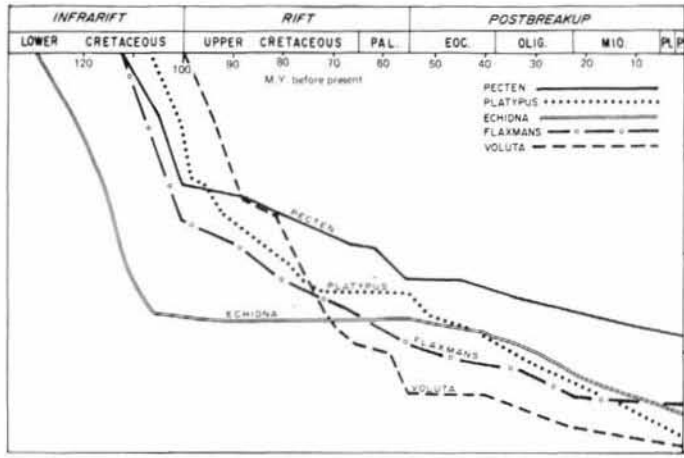
Figure 3
Cumulative subsidence or Geohistory plots for five exploration wells from Australia's southern margin (after Falvey, Mutter, 1981). Only the well total depth (T. D.) in shown. All data are corrected for compaction as described in Appendis 1, using well-specific porosity depth functions. Sealevel and palaeowater depth are not shown.

omitted for clarity. The data have been corrected for the effects of compaction and palaeowater depth (Appendix 1). The southern margin was chosen because it is the youngest (55 m.y. b.p.) in the Australian region, has thin postbreakup sedimentary cover, and an extensive, high quality data set. The five wells specifically chosen contained the most complete sections of post- and prebreakup units (although only one well, Echidna-1, contains a complete Lower Cretaceous section).

Widespread infrarift phase subsidence appears to have begun 80 m.y. before breakup. Echidna shows rapid subsidence, sharply declining towards the end of the early Cretaceous. Flaxmans, Pecten and Playpus have a similar sediment accumulation pattern beginning partway through the infrarift subsidence phase. Echidna lies landward of the depocentre and boundary fault, and shows no rift phase subsidence. The other wells show that nearer the depocentre, infrarift and rift phase subsidence is both *continuous*, and, we interpret, exponentially decreasing with time up until the breakup at 55 m.y. b.p. It is important to note that rift onset (45 m.y. before breakup) involves little discontinuity in depocentre sedimentation, but merely constrains that sedimentation to fault bounded troughs. After breakup sedimentation rates at first increase ; and then decrease with time as described by Watts and Ryan (1976). In the

vicinity of depocentres, breakup unconformities involve virtually no erosion or uplift. The greater part of the southern margin is characterised by virtually continuous subsidence over the last 135 m.y. with only a rate discontinuity at breakup.

CONTINENTAL MARGIN SUBSIDENCE MECHANISMS

Falvey (1974) proposed deep crustal metamorphism prebreakup, and thermal cooling postbreakup to explain this overall pattern of margin sedimentation and subsidence. The prebreakup metamorphic mechanism is thought to occur during rising heatflow conditions and the postbreakup cooling mechanism occurs during declining heatflow conditions. The peak thermal conditions should occur at breakup time, at the continent-ocean boundary.

The prebreakup mechanism may be explained on the metamorphic facies diagram in pressure-temperature space (Fig. 4). As heatflow rises above 0.8 HFU (33 mWm^{-2}) the continental geotherm will intersect the greenschist-amphibolite boundary at progressively shallower depths. The dewatering of the greenschist-amphibolite conversion involves a 7 to 10 % density increase. Contraction of the

Figure 4
The upper part of the figure shows the key metamorphic facies (greenschist and amphibolite) in temperature-pressure (depth) space (modified after Falvey, 1974). In a rising heatflow situation more of the lower continental crust becomes metamorphosed to a rock of about 7-10% higher density. This causes isostatic subsidence to occur which is shown affecting difference thicknesses of continental crust in the lower part of the figure.
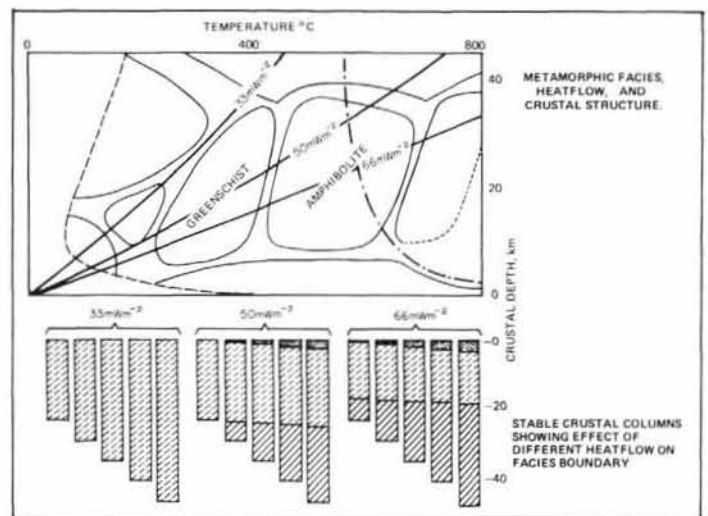
crustal column causes subsidence which eventually facilitates near sealevel sedimentation. The sediment blanket further increases the pressure and temperature conditions at depth, which enhances the isostatic multiplying factor of sedimentation. Thus basin subsidence may occur under rising heatflow conditions provided thermal expansion in the lithosphere is outpaced by metamorphic contraction in the deep crust (see Middleton, 1980). As shown in Figure 2, it is proposed that this occurs within that region of the margin which includes rift phase sedimentation. Nearer the incipient continent-ocean boundary, where peak thermal conditions will occur, lithosphere thermal expansion may eventually outpace deep crustal metamorphism. After breakup, thermal cooling and lithosphere contraction becomes the dominant mechanism of subsidence ; operating on already thinned and metamorphosed crust.

In the region of peak thermal conditions crustal anatexis may take place, giving rise to acid to intermediate volcanics, and partial melting of mantle lithosphere may also give rise to basic volcanics. Von Stackelberg et al. (1980) have recorded small quantities of rhyolite, trachyte and basalt amongst marginal to non-marine rift and marine postbreakup sediments in dredge hauls from the margins of the Exmouth and Wallaby Plateaus (off Western Australia).

It is relevant to note that where high grade Precambrian shield can be reasonably extrapolated offshore beneath the shelf, such as off southwestern Australia, there is little evidence of extensive infrarift and/or rift phase sedimentation. Crustal thinning may occur through erosion during uplift caused by rising heatflow conditions. Limited metamorphism to still higher grade might be expected where the crust is thick.

STRUCTURAL EVIDENCE OF DEEP CRUSTAL METAMORPHISM

P-wave seismic velocity may be a reasonable guide to crustal metamorphic grade (Ringwood, Green, 1966). Data on amphibolites of basaltic composition (in Christensen, 1965) give an average velocity of 7.3 ± 0.2 km/sec. and a density of 3.1 ± 0.1 gms/cm^3. Basic plutonic igneous rocks have an average velocity of 6.8 ± 0.3 km/sec. and eclogites (and probably some granulites) have an average velocity of 7.9 ± 0.3 km/sec. (Press, 1966). Thus, seismic refraction velocities in the range 7.1 to 7.5 km/sec. which are commonly observed at continental margins (Sheridan, 1969) may be associated with amphibolite grade continental crust. Velocity data from deep refraction profiles on Australia's northeast and southern margins (Ewing et al., 1970 ; Mutter, 1978 ; Talwani et al., 1979) are summarised in Figure 5. An interpreted geometry of the greenschist-amphibolite metamorphic facies boundary at a continental margin which may be typical is shown in Figure 6. The profile extends
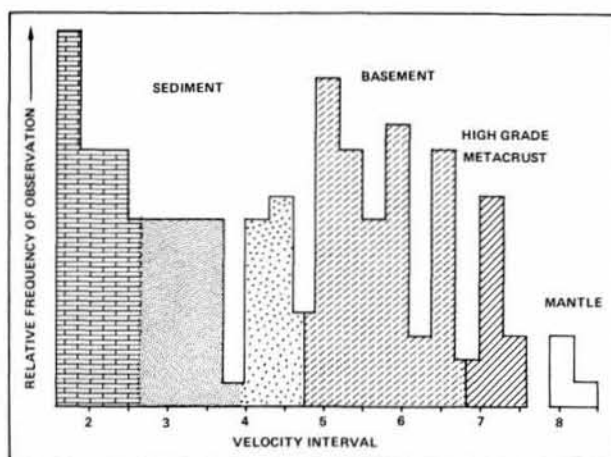

Figure 5

Histogram of the frequency of seismic refraction velocities which occur in certain refraction profiles from the Queensland Plateau (Ewing et al., 1970) and the Southern Margin (Mutter, 1978 ; Talwani et al., 1979). Data was taken from refraction probes which detected at least one layer deeper than superficial basement on the continent side of the continent-ocean boundary. The occurrence of a discrete high grade metacrustal layer in the range 7,0-7,5 km/sec. is considered statistically significant.

Figure 6

Computed two-dimensional gravity model across the Queensland Plateau. This corresponds to profile A-A' of Taylor and Falvey (1977) and extends from approximately 19°S, 148°E to 14°S, 153°E. Seismic refraction control is from Ewing et al. (1970) ; and the gravity data was collected by R/V. Vema in 1967, and is used with permission of Pr. M. Talwani. 15 m.gals regional geoid anomaly has been substracted from the observed data, and the model designed to be in regional isostatic equilibrium at 32 km. An extensive deep crustal metamorphic layer is inferred with a density of 3,05 gms/cm^3 and a velocity of 7,5 km/sec.
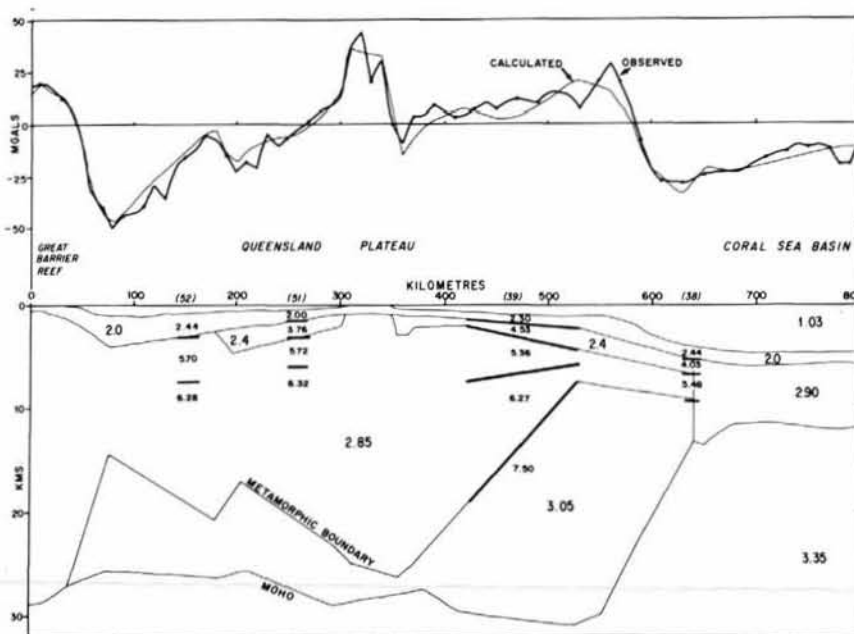
from the Coral Sea Basin across the Queensland Plateau, on Australia's northeast margin. Seismic refraction data is from Ewing *et al.* (1970). The gravity model was computed by Falvey (1972) and by Taylor and Falvey (1977) and has been slightly modified for this example. The relative isostatic load at 32 km averages zero over approximately 100 km horizontal distance. The fit of the calculated profile to the observed regional is considered quite satisfactory. The 7.5 km/sec. refractor is interpreted as the greenschist-amphibolite boundary. It rises markedly towards the continent-ocean boundary (corresponding to presumed prebreakup thermal state), and gives an almost constant Moho depth over all but the outermost part of the plateau. The amount of isostatic crustal shrinkage contained in the thickness of the deep crustal layer is approximately that required to cause the observed basement subsidence from near sealevel. Thus continental crustal extension is not necessary to produce subsidence except, in part, within a small distance from the continent-ocean boundary.

BASEMENT SUBSIDENCE MODELLING BY METAMORPHISM AND COOLING

Sleep (1971) presented a quantitative thermal cooling (lithosphere contraction) model which satisfactorily described postbreakup sedimentation. This model has been extended by Watts and Steckler (this volume), and seems an adequate description of this final phase of passive margin subsidence. However, as Figure 3 illustrates, the prebreakup sedimentation function resembles the postbreakup function. The latter is an exponential or square-root function of time, depending upon whether the thermal cooling solution or the model itself is subject to approximation. The data in Figure 3 show that the combined infrarift and rift phases of sedimentation, where they are continuous, may be described by an exponential or square-root function of time, similar to a thermal cooling model.

This raises a dilemma. Breakup time should, in principle, be the time of peak thermal conditions, since this is the time molten asthenosphere freezes out as oceanic lithosphere, up to the surface. Further, it is difficult to invoke two simple thermal cooling cycles to explain the "double exponential" subsidence function, since the breakup time does not represent significant uplift or erosion in, and near depocentres. Thus, any mechanism which describes infrarift and rift phase subsidence (near sealevel deposition) followed closely by postbreakup cooling subsidence, must involve crustal (isostatic) modification in the prebreakup period. The deep crustal metamorphism model is consistent with this observation.

Middleton (1980) formulated a relatively simple, one-dimensional model, which described the form of basement subsidence due to deep crustal metamorphism during a lithosphere heating cycle. Thermal conduction in a semi-infinite medium is described by an error function of time in both the heating and cooling case. In the cooling case, subsidence is proportional to temperature drop integrated over depth (contraction) — i.e. proportional to square-root of time. In the heating case, subsidence is proportional to temperature increase at the metamorphic facies boundary. To a first order approximation, this is also proportional to the square-root of time. Details are given in Appendix 2. Thus initial prebreakup exponential or root-time subsidence may occur in the heating cycle and a final exponential or root-time subsidence immediately follows during the postbreakup cooling cycle.

This hypothesis has been tested against the observed sedimentation pattern in Platypus-1 (Fig. 3). To allow for the effects of compaction of early infrarift sediments below the well T.D., a seismic basement (presumed top of non-compactable rocks) was picked at a depth of 5.5 km subsealevel. This represents the sediment loaded subsidence plus second order sealevel and palaeowater depth effects, and is shown in Figure 7. Basement subsidence both pre- and postbreakup was successfully modelled by introducing an anomalous temperature step function of 300°C, from 140 m.y. b.p. to 53 m.y. b.p. (approximately breakup time). A greenschist-amphibolite density contrast of 10 % was assumed. The input temperature function, and the temperature response function at 25 km depth are shown on Figure 7. The prebreakup deep crustal metamorphism model thus accurately describes the complex range of continental margin depocentre subsidence given peak thermal conditions at breakup time.
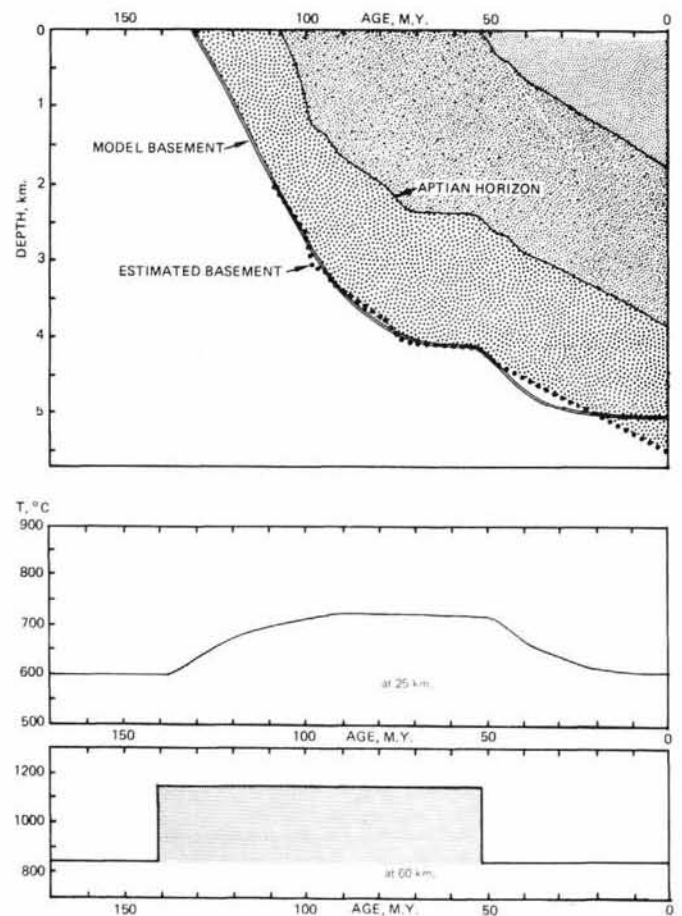

Figure 7

The upper part of the figure shows a cumulative subsidence or Geohistory plot of Shell Platypus-1 extrapolated to an earliest Cretaceous seismic basement. Infrarift, rift, postbreakup and palaeowater depth are shown. The model basement subsidence was derived assuming a thermal anomaly of 300°C, from 140 m.y. to 53 m.y. before present at 60 km depth as shown in the bottom of the figure. The consequent thermal anomaly at 25 km depth is also shown. The thermal anomaly onset produces some thermal expansion and uplift, quickly outpaced by deep crustal metamorphism and subsidence. The consequent sediment accumulation exponentially decreases with time as derived in Appendix 2. After breakup at 53 m.y.b.p. thermal cooling and contraction causes postbreakup subsidence.

PALAEOHEATFLOW MODELLING USING LEVEL OF ORGANIC METAMORPHISM

Quantitative modelling of continuous prebreakup and post-breakup basement subsidence is, in principle, possible using alternative methods of modifying the prebreakup continental crust. If the infrarift and rift stages involved crustal extension by stretching (Bott, 1971 ; McKenzie, 1978) or crustal extension by dyke injection (Burke, 1975 ; Royden *et al.*, 1980) then the complex subsidence patterns observed in Figures 3 and 7 may be contrived.

However, the thermal, or palaeoheatflow predictions of the deep crustal metamorphism model and of the crustal extension model are not the same for an equivalent sediment accumulation history. For the crustal extension model to reproduce the subsidence patterns seen in Figure 3, and maintain substantial continuity of deposition through the breakup period in depocentres, then peak heatflow would occur near the beginning of the infrarift stage (or at least be extended throughout the prebreakup period, depending upon the extension model details). This is because the extension model entails an initial rapid pull-apart in the early infrarift stage which gives rise to initial rapid deposition and high heatflow. This is followed by diminishing deposition rate and declining heatflow through most of the prebreakup and the postbreakup stages (Sclater, Cristie, 1980).

In the case of subsidence caused by deep crustal metamorphism, the subsidence rate is related to the rate of change of thermal gradient. Thus peak heatflow is reached at the end of the prebreakup subsidence stage. In both models, post-breakup subsidence entails similar declining heatflow. Thus, the metamorphism model predicts lower mean heat-flow than the extension model, particularly in the prebreakup period.

The fundamental test of the extensional and metamorphic models of prebreakup subsidence thus lies in the determination of palaeoheatflow. The integrated thermal history of a sediment is recorded in the percentage random reflectance of the coaly maceral, vitrinite (Lopatin, 1971 ; Hood *et al.*, 1975 ; Shiboaka, Bennett, 1977 ; Waples, 1980). We have extended the work of these authors and developed a quantitative technique for deriving theoretical vitrinite reflectance as a function of depth at a test well location, given an assumed palaeoheatflow function. This theory is presented in more detail in Appendix 3. The comparison of theoretical and observed vitrinite reflectance is considered an appropriate and accurate test of palaeoheatflow.

Figure 8 shows theoretical vitrinite reflectance for Platypus-1 based on an extensional and on a metamorphic prebreakup subsidence model, compared with observed data. For the metamorphic model, palaeoheatflow effectively follows the palaeotemperature at 25 km depth shown in Figure 7. For the extension model a stretching factor of only 1.8 was applied to continental crust on an already thinned litho-sphere, and the palaeoheatflow function derived from Equation 7 of McKenzie (1978). This is as low a palaeoheat-flow function as we could find for an extensional driving mechanism to the Platypus basement subsidence. The comparisons on Figure 8 clearly support the low heatflow, metamorphic subsidence model.

Further support for this conclusion may be found elsewhere. Von Stackelberg *et al.* (1980) dredged non-marine coaly and carbonaceous silts of Jurassic age from a water depth of 4.5 ± 0.7 km in the Swan Canyon, Exmouth Plateau. These late rift phase (prebreakup) coals
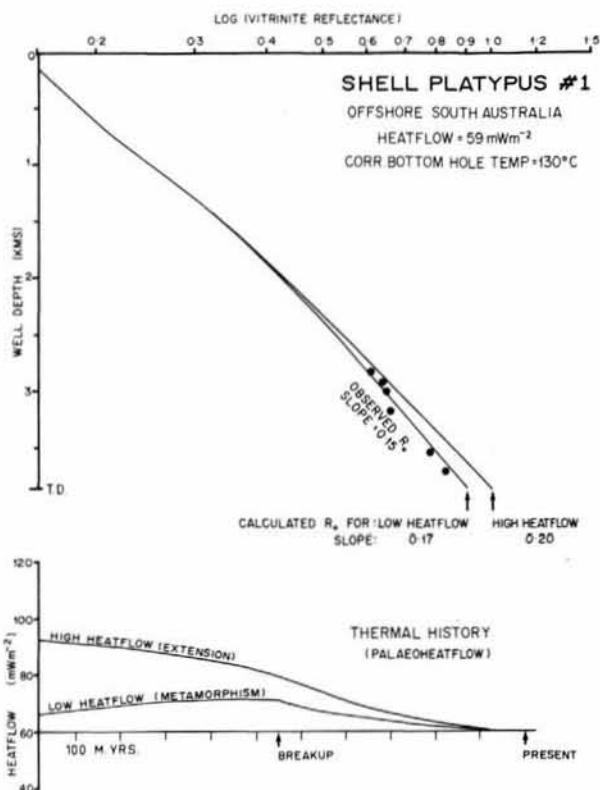

Figure 8

The upper part of the figure shows observed (log) vitrinite reflectance plotted against depth for Shell Platypus-1. Theoretical vitrinite reflectance is also shown for a low palaeoheatflow model (deep crustal metamorphism) and a high palaeoheatflow model (crust extension by stretching). The method of calculation is discussed in Appendix 3. The palaeoheatflow for the low heatflow case was derived from the model discussed in Appendix 2. The high palaeo-healtflow case was derived from Equation 7 of McKenzie (1978) using a stretching factor of 1,8 on an already thinner lithosphere.

had a vitrinite reflectance of 0.36 ± 0.02 %. It is difficult to see how such rocks could subside so far under an extensional mechanism and yet record such a low integrated thermal history.

CONCLUSIONS

The Australian continental margin presents major advantages for the study of passive margins and subsidence driving mechanisms :

1) The margin is extensive and well documented.
2) The margin is clearly divided into five segments of well defined breakup age.
3) For reasons of climate, geography and oceanography the postbreakup sediment "screen" is thin, allowing easy penetration.
4) There are extensive marginal plateaus ; the majority (if not all) of which are continental crust with virtually no postbreakup sediment.
5) A quality data base exists, mainly as a result of lease relinquishment requirements on offshore oil search.

An extensive study of most published and openfile data on the Australian margin has led us to propose that significant

subsidence occurs before breakup in non-marine or shallow water environments under relatively low heatflow conditions. Breakup unconformities are not major subareal erosion events, and depocentre basement subsidence is virtually continuous through breakup. We have correlated the presence of high refraction velocity continental crust with prebreakup deep crustal metamorphism. This model adequately describes the double exponential subsidence pattern of passive margin sediments, and the low vitrinite reflectance values in prebreakup sediments in particular.

Acknowledgements

Appendix 1

A graphical technique for reconstructing the depositional or subsidence history of a drill hole has been given by Perrier and Quiblier (1974). Their procedure has been somewhat extended by Van Hinte (1978). His method was also graphical and its interpretation referred to as "geohistory analysis". In an attempt to quantify the procedure of calculating time/cumulative well subsidence diagrams, Sclater and Christie (1980 ; Appendix A) have adopted an exponential porosity — depth relationship. We have found that in most cases such function do not fit shallower depth data particularly well. We formulate the following relationship by assuming that incremental change in porosity, $d\phi/\phi$ is proportional to change in load, dL., and the void ratio, e :

$$d\phi/\phi = - ke\, dL .$$

But,

$$e = \frac{\phi}{1-\phi}$$

and

$$L = (1 - \phi)\, dh$$

$$d\phi/\phi^2 = - k\, dh$$

$$1/\phi = 1/\phi_0 + kh \qquad (1.1)$$

where ϕ is initial (uncompacted) porosity, k is a constant, and h is depth. For sands : $\phi_0 = 0.4 - 0.5$, $k = 1.5 - 2.0$ km^{-1}

shales : $\phi = 0.5 - 0.7$, $k = 2.0 - 2.5$ km^{-1}.
An excellent approximation to the general function of Roll (1974) is $\phi = 0.53$, $k = 2.18$ km^{-1} (good to within a few percent).

Equation (1.1) makes it relatively easy to correct well data for the effects of compaction using the Perrier and Quiblier method of slices. The total amount of solid or skeletal material in a buried interval (Z_1 to Z_2) is given by :

$$h_s = \int_{Z_1}^{Z_2} (1 - \phi(h))\, dh . \qquad (1.2)$$

Integrating (1.2) by substituting (1.1) :

$$h_s = (Z_2 - Z_1) - 1/k . \ln\left[\frac{1/\phi_0 + kZ_2}{1/\phi_0 + kZ_1}\right]. \qquad (1.3)$$

This amount of skeleton is a constant. The compaction corrected thickness of this layer at an earlier depositional epoch may be calculated ; given the top (Z_3) and calculating the bottom (Z_4) :

$$Z_4 - 1/k . \ln(1/\phi_0 + kZ_4)$$
$$= Z_3 - 1/k . \ln(1/\phi_0 + kZ_3) + h_s . \qquad (1.4)$$

A simple computer iteration will solve the left hand side of (1.4) for Z_4. Thus, given the compaction parameters, and drillhole values of depth, age, and palaeowater depth a computer programme can be written which will solve equations (1.3) and (1.4) and plot the time/cumulative subsidence curves shown in figures 3, 7 and 9.

Appendix 2

Subsidence due to deep crustal metamorphism can be modelled by assuming a metamorphic density increase to occur at the greenschist facies — amphibolite facies boundary. The general method of modelling subsidence by metamorphism of the deep crust is described by Middleton (1980), where the effect of the heat absorbed by the metamorphic reactions (some 40 cal./g in the case of greenschist to amphibolite facies) is demonstrated to have negligible perturbation of the ambient geothermal gradient.
The greenschist-amphibolite facies boundary is assumed to be described by the relation :

$$T_{pb} = mz' + b, \qquad (2.1)$$

for depths of 10 to 30 km, where T_{pb} is temperature, z' is the depth to the phase boundary, and m and b are constants. The temperature distribution $T(z, t)$ in the lithosphere of thickness H with base maintained at an anomalous temperature of T_0 for $t > 0$ and surface maintained at zero temperature is given by :

$$T(z, t) = T_0 \sum_{n=0}^{\infty} \left| \text{erfc}\left(\frac{H(2n+1) - z}{(4\kappa t)^{1/2}}\right) \right.$$
$$\left. - \text{erfc}\left(\frac{H(2n+1) + z}{(4\kappa t)^{1/2}}\right) \right| + D(z), \qquad (2.2)$$

where $D(z)$ is the stable temperature distribution in the lithosphere before the thermal event, z is depth, t is time, and κ is thermal diffusivity. The base of the lithospheric slab coincides with the top of upwelled asthenospheric material of anomalous temperature T_0. Assuming for simplicity that in the present model the initial depth of the phase boundary is also H, i.e. $z' = H$ for $t = 0$, then the displacement of the

Figure 9

Graphical illustration of the method of calculating theoretical vitrinite reflectance of or a simple case where three drillhole ages are known. Top-left shows the cumulative subsidence or Geohistory plot (Van Hinte, 1978). Top-right shows a model conductivity-depth function (see text) plus a derived temperature-depth function for a given heatflow value. Centre-left gives an example (or first try) palaeoheatflow derived from a best fit lithosphere cooling model assuming a root-age function (see text). Bottom-left gives the temperature-time function derived for each of the three beds, given the preceding palaeoheatflow, conductivity and cumulative subsidence plots. Bottom-right shows the theoretical log (vitrinite reflectance) — depth plot obtained by integration (see text). Note that this plot is essentially linear as stated by Dow (1977).
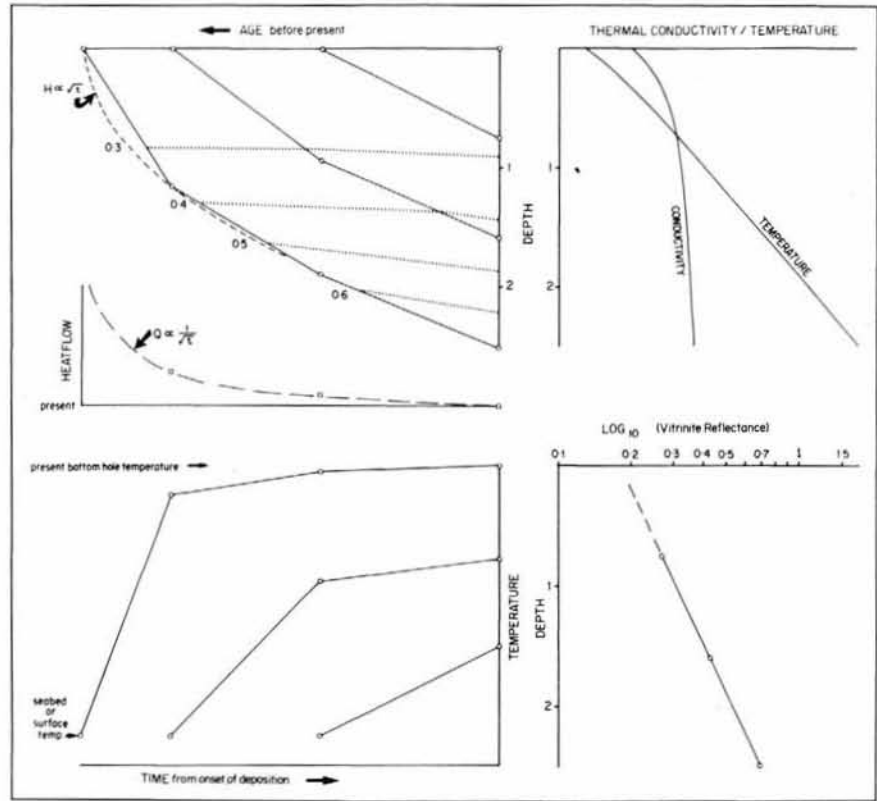
phase boundary $L(t) = H - z'$, can be found by solving (2.1) and (2.2) simultaneously with $z = z'$ for $H - z'$. We will show that $L(t)$ is proportional to the square root of time for small values of time.

In the vicinity of depths approaching H and for small values of t, equation (2.2) is well approximated by :

$$T(z, t) = T_0 \operatorname{erfc}\left(\frac{H - z}{(4\,\kappa t)^{1/2}}\right) + Gz + F,\qquad (2.3)$$

where $D(z)$ is assumed to be linear and equal to $Gz + F$. Further, for small values of $H - z'/(4\,\kappa t)^{1/2}$, equation (2.3) can be written :

$$T(z, t) = T_0 - \frac{T_0 L}{(\pi\kappa t)^{1/2}} - GL + GH + F,\qquad (2.4)$$

where $L = H - z'$ and is the expression for the temperature at the phase boundary. Equation (2.1) can be rewritten as :

$$T_{pb} = mH + b - mL,\qquad (2.5)$$

where again $L = H - z'$.
Solving (2.4) and (2.5) simultaneously for L, we find :

$$L(t) = \frac{[T_0 + H(G - m) + F - b]}{[T_0 + (\pi\kappa t)^{1/2}(G - m)]} (\pi\kappa t)^{1/2}.\qquad (2.6)$$

Typically, $G = 6.67°C/km$, $F = 300°C$, $m = 5°C/km$ and $b = 350°C$. Hence, for small t, T_0 is very much greater than $(\pi t)^{1/2}(G - m)$, and equation (2.6) is well approximated by :

$$L(t) = \frac{[T_0 + H(G - m) + F - b]}{T_0} (\pi\kappa t)^{1/2}.\qquad (2.7)$$

Equation (2.7) states that for small times $L(t)$ is proportional to the square root of time.

Displacement of the earth's surface $l(t)$ due to the density change involved in the movement of the phase boundary a displacement $L(t)$ is :

$$l(t) = \left(\frac{\rho_a - \rho_g}{\rho_g}\right) L(t),\qquad (2.8)$$

where ρ_a is the density of the amphibolite facies rock and ρ_g is the density of the greenschist facies rock. $l(t)$ is also proportional to the square root of time.

Acting against this subsidence, $l(t)$, is uplift due to thermal expansion of the lithosphere entailed by the heating during the thermal event. This uplift $h(t)$ is obtained from the integral :

$$\begin{aligned}h(t) &= \alpha T_0 \int_0^H \operatorname{erfc}\left(\frac{H - z}{(4\,\kappa t)^{1/2}}\right) dz\\ &= \alpha T_0 (4\,\kappa t)^{1/2}\left[(\pi)^{-1/2} - \operatorname{ierfc}\left(\frac{H}{(4\,\kappa t)^{1/2}}\right)\right],\end{aligned}\qquad (2.9)$$

where α is the coefficient of thermal expansion. In the small time approximation, $\operatorname{ierfc}[H/(4\,t)^{1/2}]$ is effectively zero as $(4\,\kappa t)^{1/2} < H$. Equation (2.9) becomes :

$$h(t) = \alpha T_0 \left(\frac{4\,\kappa t}{\pi}\right)^{1/2}.\qquad (2.10)$$

Displacement $S_b(t)$ of the sedimentary basin basement caused by the metamorphism mechanism is given by :

$$S_b(t) = l(t) - h(t),\quad \text{for}\quad h(t) > l(t)$$
$$S_b(t) = \frac{\rho_m}{\rho_m - \rho_s}[l(t) - h(t)],\quad \text{for}\quad h(t) < l(t),\qquad (2.11)$$

where the negative sign indicates uplift, ρ_m is the density of the mantle and ρ_s is the density of loading sediment. Equation (2.11) applies for sediment loading to sea-level, neglecting compaction of sediment.

Subsidence of the sedimentary basin basement given in (2.11) is linearly related to $t^{1/2}$, the square root of time after beginning of subsidence. For large times, the expression for subsidence departs from the $t^{1/2}$ form to a function of exponential form.

Appendix 3

According to theoretical chemistry, the rate of change of coalification should vary with temperature as defined by the Arrhenius equation :

$$k = A \exp(-E/RT),\tag{3.1}$$

where K is reaction rate constant, A is the frequency factor, E is the activation energy, R is the gas constant, and T is absolute temperature. In practice, however it is not possible to describe observed coalification by such an expression using constant A and E. Most authors have constructed nomograms, etc., using empirical relationships. Hood et al. (1975) however, imposed equation (3.1) on their diagram which relates level of organic metamorphism (LOM) to inverse absolute temperature and "effective time". The slopes of constant LOM lines on their Figure 3 are proportional to activation energy. That figure shows that E varies with temperature or LOM such that the reaction rate, or rate of change of degree of coalification doubles with each 10°C (10.2°C) increase in temperature. This relationship had been proposed by Lopatin (1971) and adopted by Shiboaka and Bennett (1977) in the construction of their nomogram.

The frequency factor is also a possible variable in higher order versions of equation (3.1). However suitable expressions do not appear to be theoretically justifiable. Thus, we have chosen to quantify the empirical relationship noted above :

reaction rate,

$$k = \frac{dc}{dt},\tag{3.2}$$

where c is an, as yet undefined measure of coalification. At constant cooking time :

$$\frac{\partial K}{k} \propto \partial T$$

i.e. $k = a\,e^{\alpha T}$, (3.3)

k will double for a 10.2°C increment in temperature when $\alpha = \ln(2)/10.2$ (i.e., 0.068).
Combining equations (3.2 and 3.3) :

$$c = \int_0^t k\, dt$$

$$= a \int_0^t e^{\alpha T}\, dt\tag{3.4}$$

$$= a \int_0^t 2^{T/10.2}\, dt,$$

i.e. $c/a \doteq$ TTI ; the time-temperature index defined by Lopatin (1971) and Waples (1980).
If we define "effective time", t_e as the time for which cooking at a temperature T_{max} will produce the same coalification then :

$$c = at_e\, e^{\alpha T_{max}}\tag{3.5}$$

where

$$t_e = e^{-\alpha T_{max}} \int_0^{T_{max}} e^{\alpha T}\, dT\ .\tag{3.6}$$

Effecive time is thus an exponentially weighted mean cooking time. Differentiating equation (3.6) with respect to time :

$$\frac{dt_e}{dt} = 1 - \alpha t_e \frac{dT}{dt}\ .\tag{3.7}$$

This is the mathematical expression of the graphical procedure described by Shiboaka and Bennett (1977, Fig. 6). To demonstrate the relationship between this nomogram and that of Hood et al. (1975, Fig. 3) consider the case where temperature is a slow, monotonically increasing function time. Then, $\frac{dt_e}{dt}$ in equation (3.7) should approach zero, and :

$$t_e = \frac{1}{\alpha} \cdot \frac{dt}{dT_{max}}\ .$$

Effective time is then the time that temperature has been with $(1/\alpha)$°C of the maximum temperature (i.e. 14.7°C). Hood et al. (apparently arbitrarily) defined effective time as the time within 15°C of maximum temperature. Thus the nomograms of Shiboaka and Bennett, and Hood et al. are equivalent.

Degree of coalification is not a directly measurable quantity. Hood et al. (1975) defined levels of organic metamorphism as a function of t_e and T_{max} but Shiboaka and Bennett used the directly measurable vitrinite reflectance (or percentage mean or random optical reflectance of vitrinite). Hood et al. provided a further nomogram relating vitrinite reflectance to LOM. We have empirically calibrated equation (3.5) to both data sets and concluded that :

$$R_0^{5.635} = C = at_e\, e^{\alpha T_{max}}$$

where

$$a = 2.7 \times 10^{-6} \quad \text{for} \quad t_e \text{ in m. yrs}\ .\tag{3.8}$$

Vitrinite reflectance modelling

To apply equation (3.8) to making model predictions of vitrinite reflectance, a quantitative expression for temperature as a function of time is required for all model depth points. To do this it is necessary to reconstruct the thermal state and depositional history of a drill hole or test location. The latter problem is resolved in Appendix 1 and shown in Figure 9. The former is resolved by considering both thermal conductivity and palaeoheatflow (also see Fig. 9). Ideally, thermal conductivity measurements should be available from a drill hole, so as to accurately determine temperature distribution between surface and the bottom hole temperature now, and at earlier times. In practice, such measurements are not made and we must make do with best estimates of conductivity. For sediments in situ the value of thermal conductivity varies between 2×10^{-3} and

12×10^{-3} cal. cm^{-1}.$^{\circ}$C^{-1}. It increases markedly with decreasing porosity (i.e. depth of burial) and decreases with increasing temperature (also with depth). We have found that a suitable thermal conductivity/depth function is given by :

$$K = K_m - (K_m - K_o) \exp(-\beta h), \qquad (3.9)$$

where K_m is maximum thermal conductivity at zero porosity and deep basin temperatures ; K_o is minimum porosity at surface porosity and temperature ; and β is a constant giving the exponential rate of change with depth, h, between these limits (see also Sclater, Christie, 1980, Fig. B3). Where compaction is slow and temperature gradient effects high, $\beta = 0.5 - 0.7$ km^{-1}. Where compaction is rapid and temperature gradient effects low, $\beta = 1.2 - 1.4$ km^{-1}.

To calculate a temperature/depth function, assume zero heat generation from within the sediment pile. The heatflow equation becomes :

$$Q = K \frac{\partial T}{\partial h}, \qquad (3.10)$$

where Q is heatflow positive upwards, and h is depth positive downwards.

Combining equations (3.9) and (3.10) and integrating with respect to depth :

$$T = T_o + \frac{Q}{K_m}\left[h + \frac{1}{\beta} \ln\left[\frac{K_m}{K_o} - \frac{K_m - K_o}{K_o} \exp(-\beta h)\right]\right], \qquad (3.11)$$

where T_0 is surface or seabed temperature. If it is assumed : that β and K_0 do not vary much regardless which part of the sedimentary section is considered ; that β and K_m do not vary much with changes in Q ; and that T_0 does not vary ; then it is possible to apply equation (3.11) at all past times on the time/cumulative subsidence plot (Fig. 9). We have found this a quite adequate procedure, and one which is cerainly simple, and gives excellent approximations.

The heatflow may be a variable function of geological time. In fact, in a normal sedimentary basin which forms by lithosphere cooling and contraction (Sleep, 1971) heatflow would be expected to decrease with increasing time and sedimentary accumulation. Taking the example of the cooling infinite half space model summarized by Watanabe et al. (1977) :

$$Q(t) = \frac{KT_A}{(\pi \kappa t)^{1/2}} \qquad (3.12)$$

$$H(t) = \frac{2 \rho_m \alpha T_A}{(\rho_m - \rho_s)} \left(\frac{\kappa t}{\pi}\right)^{1/2}, \qquad (3.13)$$

where T_A is the anomalous temperature ; k is thermal diffusivity ; H is sedimentary thickness ; ρ_s sediment density and ρ_m is mantle density ; and α is the coefficient of thermal expansion. In this case programme protection is required against the heatflow singularity at zero time. The common unknown here is T_A which may be eliminated :

$$Q(t) = \frac{C_o(\rho_m - \rho_s)}{2 \alpha \rho_m} \cdot \frac{H(t)}{t}, \qquad (3.14)$$

where C_p is specific heat. Equation (3.14) provides a point-by-point estimation of heatflow after time zero. We have preferred to carry out a least squares fit to cumulative

subsidence data using equation (3.13) and then evaluate anomalous heatflow using equation (3.12). Either way, the cumulative subsidence of the basin at the drillhole location provides the first approximation of palaeoheatflow (Fig. 9). At this point is possible to generate a temperature/time function for each bed of known age and depth (and palaeowater depth) in the drill hole or test location. This applies equations (1.3 ; 1.4 ; 3.11) and equations (3.12 ; 3.13 or 3.14) or an independent estimate of Q(t) in a computer programme of sufficient simplicity to be run on any minicomputer. The stylized output is shown in Figure 9.

To compute theoretical vitrinite reflectance, the integral in equation (3.4) is calculated numerically, and summed. Let temperature rise linearly over a short interval from T_1 to T_2 (time interval t_1 to t_2 from the onset of deposition). Then :

$$I = \int_{t_1}^{t_2} e^{\alpha T} dt,$$

the slope of the temperature/time function is :

$$\frac{dt}{dT} = \frac{t_2 - t_1}{T_2 - T_1} = \gamma, \quad I = \gamma \int_{T_1}^{T_2} e^{\alpha T} dT = \frac{\gamma}{\alpha}(e^{\alpha T_2} - e^{\alpha T_1}). \qquad (3.15)$$

The value of the integral is summed for all time increments after the onset of deposition of the particular bed. The value of the sum is then converted to vitrinite reflectance using equation (3.8) :

$$R_o = (a.I)^{1/5.635}$$

Contours of equal vitrinite reflectance may be plotted on the time/cumulative subsidence curve (Fig. 9) and current (present day) values of vitrinite reflectance may be directly compared with drillhole observation. Palaeoheatflow may then be modified to produce a better fit between theory and observation with the concomitant prediction of palaeomaturation.

An apparent weak point in the computation is equation (3.11). In practice, however, calculated vitrinite reflectance is not particularly sensitive to some variation in K_o, K_m and β. Since current bottom hole and surface temperature are fixed, variations in these parameters affect only the curvature of the (log) vitrinite reflectance/depth function between two essentially fixed points. Changes in palaeoheatflow produce changes in the gradient of the (log) vitrinite reflectance vs. depth curve. Indeed that gradient has a straightforward theoetical significance in certain simple cases. Dow (1977) noted that generally the slope of the log (R_o) vs. depth function was essentially constant. This can be demonstrated given a constant deposition rate, $S(=\frac{dh}{dt})$, and constant palaeoheatflow (i.e. $T = \frac{\varphi}{\kappa}.h$.

$$R_o^* = \frac{a}{S}\int_0^h e^{(\frac{\varphi}{\kappa})h} dh = \frac{aK}{\alpha SQ}(e^{(\frac{\varphi}{\kappa})h} - 1).$$

Taking the $\log_{10}$ of both sides and differentiating :

$$\frac{d}{dh}\log_{10} R_o = \log_{10} e \cdot \frac{\alpha}{\varepsilon} \cdot \frac{Q}{K}$$

$$= 0.005 \, \partial T/\partial h. \qquad (3.16)$$

Thus slope in proportional to thermal gradient in the simplest case.

REFERENCES

Bott M. P. H., 1971. Evolution of young continental margins and formation of shelf basins, *Tectonophysics*, 11, 319-327.

Burke K., 1975. Hot spots and anlacogens of the European margin : Leicester/Shropshire ; Oslo/Fren ; Atno, *Geol. Soc. Am. Abstr.*, 7, 34-35.

Christensen N., 1965. Compressional wave velocities in metamorphic rocks at pressures to 10 kilobars, *J. Geophys. Res.*, 70, 24, 6147-6164.

Deighton I., Falvey D. A., Taylor D. J., 1976. Depositional environments and geotectonic framework ; southern Australia continental margin. *Aust. Petrol. Explor. Assoc. J.*, 16, 25-36.

Dewey J. F., Bird J. M., 1970. Mountain belts and the new global tectonics, *J. Geophys. Res.*, 75, 2625-2647.

Dow W. G., 1977. Kerogen studies and geological interpretations, *J. Geochem. Explor.*, 7, 79-99.

Ewing M., Hawkins L. V., Ludwig W. J., 1970. Crustal structure of the Coral Sea, *J. Geophys. Res.*, 75, 11, 1953-1962.

Falvey D. A., 1972. The nature and origin of marginal plateaux and adjacent ocean basins off Northern Australia, *Ph. D. thesis, Univ. N.S.W.* (unpubl.), 238 p.

Falvey D. A., 1974. The development of continental margins in plate tectonic theory, *Aust. Petrol. Explor. Assoc. J.*, 14, 95-106.

Falvey D. A., Mutter J. C., 1981. Regional plate tectonics and the evolution of Australia's passive continental margins, *Bur. Miner. Resour. J. Aust. Geol., Geophys.*, 6, 1-29.

Hood A., Gutjahr C. C. M., Heacock R. L., 1975. Organic metamorphism and the generation of petroleum, *Am. Assoc. Petrol. Geol. Bull.*, 59, 986-996.

Lopatin N. V., 1971. Temperature : geological time as coalification factors (in Russian), *Akad. Nauk SSR Izv., Ser. Geol.*, 3, 95-106.

McKenzie D., 1978. Some remarks on the development of sedimentary basins, *Earth Planet. Sci. Lett.*, 40, 25-32.

Middleton M. F., 1980. A model of intracratonic basin formation, entailing deep crustal metamorphism, *Geophys. J. R. Astron. Soc.*, 61, 1-14.

Mutter J. C., 1978. An analysis of the Mesozoic-early Cenozoic rifting history of Australia and Antarctica, *M. Sci. thesis, Univ. Sydney* (unpubl.), 223 p.

Pettier R., Quiblier J., 1974. Thickness changes in sedimentary layers during compaction history ; methods for quantitative evaluation, *Am. Assoc. Petrol. geol. Bull.*, 58, 3, 507-520.

Press F., 1966. Seismic velocities, in : edited by S. P. Clark, *Handbook of physical constants, Geol. Soc. Am. Mem.*, 97, 195-218.

Ringwood A. E., Green D. H., 1966. Petrological nature of the stable continental crust, edited by J. S. Steinhart, in : *The earth beneath the continents, Am. Geophys. Union Geophys. Monogr.*, 10, 611-619.

Roll A., 1974. Longterm compaction of sedimentary rocks and consequences — a review (in German), *Geol. Jahrb., Ser. A*, 14, 76 p.

Royden L., Sclater J. G., Von Herzen R. P., 1980. Continental margin subsidence and heat flow : important parameters in formation of petroleum hydrocarbons, *Am. Assoc. Petrol. Geol. Bull.*, 64, 2, 173-187.

Sclater J. G., Christie P. A. F., 1980. Continental stretching : an explanation of the post-mid-Cretaceous subsidence of the central North Sea Basin, *J. Geophys. Res.*, 85, B7, 3711-3739.

Sheridan R. E., 1969. Subsidence of continental margins, *Tectonophysics*, 7, 3, 219-229.

Shiboaka M., Bennett A. J. R., 1977. Patterns of diagenesis in some Australian sedimentary basins, *Aust. Petrol. Explor. Assoc. J.*, 17, 1, 58-63.

Sleep N. H., 1971. Thermal effects of the formation of Atlantic continental margins by continental breakup, *Geophys. J. R. Astron. Soc.*, 24, 325-350.

Talwani M., Mutter J., Houtz R., Konig M., 1979. The crustal structure and evolution of the area underlying the magnetic quiet zone on the margin south of Australia, in : *Geological and geophysical investigations of continental margins*, edited by J. S. Watkins, L. Montadert and P. W. Dickerson, *Am. Assoc. Petrol. Geol. Mem.*, 29, 151-175.

Taylor L. W. H., Falvey D. A., 1977. Queensland Plateau and Coral Sea basin ; stratigraphy, structure and tectonics, *Aust. Petrol. Explor. Assoc. J.*, 17, 13-29.

Van Hinte J. E., 1978. Geohistory analysis-application of micropaleontology in exploration geology, *Am. Assoc. Petrol. Geol. Bull.*, 62, 2, 201-222.

Veevers J. J., 1980. Australian rifted margins, in : Geodynamics of seismically inactive continental margins, edited by R. A. Scrutton, Final Rep. I.G.C. W.G. 8, Am. Geophys. Union, Washington, D.C., in press.

Von Stackelberg U., Exon N. F., Von Rad U., Quilty P., Shafik S., Beiersdorf H., Seibertz E., Veevers J. J., 1980. Geology of the Exmouth and Wallaby Plateaus off northwest Australia : sampling of seismic sequences, *Bur. Miner. Resour. J.*, 5, 113-140.

Waples D. W., 1980. Time and temperature in petroleum formation : application of Lopatin's method to petroleum exploration, *Am. Assoc. pet. Geol. Bull.*, 64, 6, 916-926.

Watanabe T., Langseth M. G., Anderson R. N., 1977. Heat flow in back-arc basins of the Western Pacific, in : Island arcs, deep sea trenches, and back-arc basins, *Maurice Ewing Ser.*, I, Am. Geophys. Union, 419-427.

Watts A. B., Ryan W. B. R., 1976. Flexure of the lithosphere at continental margin basins, *Tectonophysics*, 36, 25-44.